Am J Physiol Regul Integr Comp Physiol 315: R1003–R1016, 2018.
First published September 5, 2018; doi:10.1152/ajpregu.00096.2018.

RESEARCH ARTICLE | *Physical Activity and Inactivity*

Acute HIIE elicits similar changes in human skeletal muscle mitochondrial H_2O_2 release, respiration, and cell signaling as endurance exercise even with less work

Adam J. Trewin,[1] Lewan Parker,[1,2] Christopher S. Shaw,[1,2] Danielle S. Hiam,[1] Andrew Garnham,[1,2] Itamar Levinger,[1,3] Glenn K. McConell,[1] and Nigel K. Stepto[1,3,4]

[1]*Institute for Health and Sport, Victoria University, Melbourne, Australia;* [2]*Institute for Physical Activity and Nutrition, School of Exercise and Nutrition Sciences, Deakin University, Victoria, Australia;* [3]*Australian Institute for Musculoskeletal Science, Department of Medicine, Western Health, Melbourne Medical School, The University of Melbourne, Melbourne, Victoria, Australia; and* [4]*Monash Centre of Health Research and Implementation, School of Public Health and Preventative Medicine, Monash University, Clayton, Victoria, Australia*

Submitted 9 April 2018; accepted in final form 28 August 2018

Trewin AJ, Parker L, Shaw CS, Hiam DS, Garnham A, Levinger I, McConell GK, Stepto NK. Acute HIIE elicits similar changes in human skeletal muscle mitochondrial H_2O_2 release, respiration, and cell signaling as endurance exercise even with less work. *Am J Physiol Regul Integr Comp Physiol* 315: R1003–R1016, 2018. First published September 5, 2018; doi:10.1152/ajpregu.00096.2018.—It remains unclear whether high-intensity interval exercise (HIIE) elicits distinct molecular responses to traditional endurance exercise relative to the total work performed. We aimed to investigate the influence of exercise intensity on acute perturbations to skeletal muscle mitochondrial function (respiration and reactive oxygen species) and metabolic and redox signaling responses. In a randomized, repeated measures crossover design, eight recreationally active individuals (24 ± 5 yr; $\dot{V}O_{2peak}$: 48 ± 11 ml·kg^{-1}·min^{-1}) undertook continuous moderate-intensity [CMIE: 30 min, 50% peak power output (PPO)], high-intensity interval (HIIE: 5×4 min, 75% PPO, work matched to CMIE), and low-volume sprint interval (SIE: 4×30 s) exercise, ≥7 days apart. Each session included muscle biopsies at baseline, immediately, and 3 h postexercise for high-resolution mitochondrial respirometry (JO_2) and H_2O_2 emission (JH_2O_2) and gene and protein expression analysis. Immediately postexercise and irrespective of protocol, JO_2 increased during complex I + II leak/state 4 respiration but JH_2O_2 decreased ($P < 0.05$). AMP-activated protein kinase and acetyl co-A carboxylase phosphorylation increased ~1.5 and 2.5-fold respectively, while thioredoxin-reductase-1 protein abundance was ~35% lower after CMIE vs. SIE ($P < 0.05$). At 3 h postexercise, regardless of protocol, JO_2 was lower during both ADP-stimulated state 3 OXPHOS and uncoupled respiration ($P < 0.05$) but JH_2O_2 trended higher ($P < 0.08$) and *PPARGC1A* mRNA increased ~13-fold, and peroxiredoxin-1 protein decreased ~35%. In conclusion, intermittent exercise performed at high intensities has similar dynamic effects on muscle mitochondrial function compared with endurance exercise, irrespective of whether total workload is matched. This suggests exercise prescription can accommodate individual preferences while generating comparable molecular signals known to promote beneficial metabolic adaptations.

exercise; mitochondria; muscle; reactive oxygen species

INTRODUCTION

Exercise is a front line strategy for the improvement of metabolic health and the prevention of numerous chronic diseases (21). Therefore, it is of clinical and public health relevance to understand the efficacy of various exercise modalities. Whether high-intensity interval exercise (HIIE) elicits similar or even greater beneficial metabolic adaptations than traditional endurance type exercise remains unclear. In particular, there are conflicting reports regarding whether skeletal muscle metabolic perturbations and consequent adaptive responses are proportional to the intensity of an exercise bout when total work performed is controlled (3, 12, 18, 40). Moreover, the precise mechanisms that underlie these adaptive responses remain incompletely understood.

Increases in content and/or respiratory function of skeletal muscle mitochondria represent an important adaptive response to regular aerobic exercise training (16). Despite this, the acute effects of a single bout of exercise on mitochondrial function remain relatively less studied. Mitochondrial bioenergetics (i.e., rates of ATP synthesis via oxidative phosphorylation) are regulated in response to exercise induced perturbations (i.e., PO_2, pH, Ca^{2+}, ATP, and NADH status). This can occur via complex cellular signaling events, activity of rate-limiting enzymes such as pyruvate dehydrogenase upstream of the mitochondrial electron transport system (ETS), and conceivably also by posttranslational modifications to ETS proteins, although the latter has not specifically been demonstrated under exercise conditions (7, 28, 33). The mitochondrial ETS also intrinsically generates reactive oxygen species (ROS) in the form of the superoxide anion ($O_2^{\cdot -}$), which is dismutated spontaneously or more rapidly by superoxide dismutase (SOD) to hydrogen peroxide (H_2O_2) (46). The main sites of $O_2^{\cdot -}$/H_2O_2 generation during exercise are considered to be of nonmitochondrial origin such as NADPH oxidase and xanthine oxidase (49, 55, 71), yet under basal conditions mitochondria are a primary source of $O_2^{\cdot -}$/H_2O_2 (24, 55). Therefore, as the skeletal muscle cellular environment returns toward basal conditions during recovery from acute exercise, mitochondria may not only rapidly revert back to being the primary source of $O_2^{\cdot -}$/H_2O_2 but additionally have altered rates of $O_2^{\cdot -}$/H_2O_2

Address for reprint requests and other correspondence: **N.** K. Stepto, College of Sport and Exercise Science, Victoria Univ., PO Box 14428, Melbourne, Victoria 8001, Australia (e-mail: Nigel.Stepto@vu.edu.au).

generation. We recently reported altered skeletal muscle mitochondrial respiratory function immediately postexercise in well-trained humans (37) as well as altered postexercise mitochondrial H_2O_2 emission in humans who are obese (66). However, to our knowledge, no study has investigated the acute effects of exercise intensity on mitochondrial function in human skeletal muscle. It is conceivable that differential mitochondrial responses to acute exercise may occur depending on intensity, since higher exercise intensity requires recruitment of a greater proportion of fast-twitch muscle fibers, whose mitochondria have been shown to have distinct functional characteristics (1).

The physiological implications of altered mitochondrial respiration and ROS emission in the hours postexercise are that numerous exercise-mediated adaptive responses in muscle are known to be redox sensitive (31, 53, 57, 67). Redox-sensitive signal transducers include p38 mitogen-activated protein kinase (MAPK) and AMP-activated protein kinase (AMPK) (19, 29, 30). These can promote mitochondrial biogenesis signaling via peroxisome proliferator-activated receptor-γ coactivator-1α (PGC1α; encoded by the gene *PPARGC1A*) (4, 60) as well as the upregulation of antioxidant capacity via transcription factors such as nuclear factor erythroid 2-related factor 2 (NRF2; encoded by the gene *NFE2L2*) (15). Downstream transcriptional targets of NRF2 include genes that encode enzymes critical for cellular redox homeostasis including SOD, glutathione peroxidase (GPX), thioredoxin (TRX), peroxiredoxin (PRDX), and thioredoxin reductase (TXNRD) (15). Additional regulation of postexercise mitochondrial $O_2^{\cdot-}/H_2O_2$ generation may occur via mitochondrial membrane remodeling processes (fission and fusion) via dynamin-related protein 1 (DRP1) and mitofusin (MFN2), respectively (2, 52), along with uncoupling protein-3 (UCP3), which upon activation can dissipate inner mitochondrial membrane potential to mitigate $O_2^{\cdot-}/H_2O_2$ generation (41). Taken together, altered patterns of mitochondrial $O_2^{\cdot-}/H_2O_2$ emission may have important downstream effects on a range of redox-sensitive adaptive processes in the hours following exercise (31).

Therefore, the aim of this study was to test the hypothesis that when total work performed is accounted for, higher exercise intensity leads to greater postexercise perturbations to skeletal muscle mitochondrial function (respiration and H_2O_2 emission), along with gene and protein responses related to key metabolic adaptations and redox homeostasis in young, healthy humans.

METHODS

Participants

Eight young, healthy and recreationally active individuals (6 males, 2 females) participated in this study (means ± SD; age: 24.5 ± 5.5 yr.; height: 179 ± 8 cm; weight: 79.4 ± 6.0 kg; body mass index: 24.8 ± 2.7 kg/m^2; and $\dot{V}O_{2peak}$: 48.4 ± 11.2 ml·kg^{-1}·min^{-1}) as reported recently (50, 51). All volunteers provided written informed consent after screening for contraindications to exercise via a health assessment questionnaire. Potential participants for this study were excluded if they were currently smoking, had musculoskeletal or other conditions that prevented daily activity, had symptomatic or uncontrolled metabolic or cardiovascular disease, or (females) were taking oral contraception. This study was approved by and conducted in accordance with the Victoria University Human Research Ethics Committee.

Experimental Design

Participants visited the Victoria University exercise physiology laboratory on four occasions. An initial visit involved screening and a graded cycling exercise test to determine $\dot{V}O_{2peak}$ and subsequent exercise workloads to which participants were then familiarized. Three experimental trials were then conducted using a crossover study design. Trial order was randomized using the Microsoft Excel list randomize function. Trials were conducted 7–14 days apart for males and 28 days apart for females during the early follicular phase of the menstrual cycle to control for ovarian hormone fluctuations. In each of the three experimental trials, muscle biopsy samples were collected at baseline (BASE), immediately postexercise (EX), and 3 h postexercise (3HR).

Dietary and exercise control. Participants reported to the laboratory in an overnight-fasted state. Participants recorded all food consumed in that 24-h period in a food diary and abstained from alcohol and caffeine for 48 h and structured exercise for 24 h before each experimental trial. Photocopies of the food diary were returned to participants who were instructed to replicate this diet for the second and third visits. One liter of drinking water was provided ad libitum to be consumed during and after exercise but matched between trials.

Exercise protocols. All exercise sessions were performed on an electrically braked Velotron cycle ergometer (Racermate, Seattle, WA). Participants initially performed a graded exercise test protocol to determine peak power output (PPO) and peak oxygen uptake ($\dot{V}O_{2peak}$). Briefly, the test started at 50 W and increased by 25 W each minute until perceived exhaustion was achieved as indicated by volitional cessation of cycling, or a pedaling cadence decreasing to below 60 rpm despite strong verbal encouragement. PPO was defined as the final complete stage, plus the fraction of the incomplete stage (26). Expired gases were collected throughout the test, and $\dot{V}O_{2peak}$ was determined with an online gas collection system (Moxus Modular VO_2 System; AEI Technologies, Pittsburgh, PA) calibrated as per the manufacturer's instructions. Heart rate was measured using a Polar heart rate monitor (Polar Electro). In the same visit after adequate recovery, participants were then familiarized with the experimental trial exercise protocols and workloads. One of the three exercise sessions were performed in each experimental trial. The continuous moderate-intensity exercise (CMIE) was performed at 50% of PPO for 30 min. The high-intensity interval exercise (HIIE) protocol consisted of 5× 4-min intervals at 75% PPO interspersed with 1-min passive recovery and was matched for the total kilojoules of work performed in the CMIE protocol. The sprint exercise session (SIE) consisted of 4× 30-s maximal sprint cycling efforts, with 4.5-min passive recovery intervals. The SIE session was not matched to CMIE/HIIE because it would be unrealistic for participants to perform an equal volume of sprint exercise given its physical demand. For the SIE exercise session, pedaling resistance was determined as a torque factor relative to body mass, optimized during the familiarization session to achieve a pedaling cadence throughout each interval of ~100–120 rpm at the beginning of the 30-s bout without decreasing below ~40–50 rpm at the end. Verbal encouragement was given throughout.

Muscle biopsy sampling. Muscle samples were obtained from the middle third of the vastus lateralis muscle using the percutaneous needle biopsy technique as previously described (51). Briefly, after injection of a local anesthetic into the skin and fascia (1% xylocaine; Astra Zeneca), a small incision was made and a muscle sample taken (~120 mg) using a Bergström biopsy needle with suction. Each biopsy was taken from a separate incision ~1 cm proximal from the previous biopsy. Muscle samples were dissected free of any visible connective tissue then one portion frozen in liquid nitrogen and stored at −80°C and another placed in ice-cold BIOPS preserving solution for mitochondrial functional analyses (see *Preparation of permeabilized muscle fibers*).

Preparation of permeabilized muscle fibers. To "capture" the acute regulatory effects of exercise on mitochondrial function, immediately after the biopsy, muscle fiber bundles were placed into ice-cold preserving solution (BIOPS; containing in mM: 7.23 K_2EGTA, 2.77 CaK_2EGTA, 5.77 Na_2ATP, 6.56 $MgCl_2{\cdot}6H_2O$, 20 taurine, 15 phosphocreatine, 20 imidazole, 0.5 dithiothreitol, and 50 K^+-MES at pH 7.1) and then prepared as per our previous work (66). Briefly, a small portion of muscle fibers were mechanically separated then transferred to ice-cold BIOPS supplemented with saponin (50 μg/ml) for 30 min with agitation. This was followed by agitation in ice-cold respiration buffer (MiR05; in mM: 0.5 EGTA, 10 KH_2PO_4, 3 $MgCl_2{\cdot}6H_2O$, 60 lactobionic acid, 20 taurine, 20 HEPES, 110 D-sucrose, and 1 mg/ml bovine serum albumin at pH 7.1). Two portions of the fiber bundles were blotted on filter paper for 5 s, and wet-weight mass was recorded using a microbalance (3–4 mg wet wt per replicate).

Mitochondrial respiration and hydrogen peroxide emission assay. To determine mitochondrial function and concomitant ROS emitting potential in the form of H_2O_2 ($J_{H_2O_2}$), permeabilized muscle fiber bundles were assessed in duplicate using a high resolution respirometer (Oxygraph O2k; Oroboros Instruments, Innsbruck, Austria) in respiration buffer MiR05 as per our previous work (62, 66). Briefly, a substrate, uncoupler, inhibitor titration (SUIT) protocol was performed at 37°C with O_2 concentration maintained between 300 and 500 nmol/ml. Specifically, sequential titrations of substrates were added first to assess mitochondrial complex I leak ($LEAK_{CI}$) with malate (2 mM) and pyruvate (10 mM), followed by succinate (10 mM) to assess complex II ($LEAK_{CI+II}$) state 4 respiration. Oxidative phosphorylation (state 3 respiration) supported by CI + II substrates ($OXPHOS_{CI+II}$) was then determined with titrations of ADP at 0.25, 1, and 5 mM, the latter being considered a saturating concentration since it did not lead to significantly greater J_{O_2} rates compared with 1 mM. Cytochrome *c* (10 μM) was added to confirm membrane integrity (<15% increase in O_2 flux) and then peak uncoupled respiratory flux was measured after 2–4 titrations of 25 nM carbonyl cyanide *p*-trifloromethoxyphenylhydrazone (FCCP) to assess maximal capacity of the electron transfer system supported by convergent CI and CII substrate input (ETS_{CI+II}). Inhibitors of specific complexes were then applied: rotenone (1 μM) to inhibit CI resulting in ETS supported only by CII substrate flux (ETS_{CII}), followed by the CIII inhibitor antimycin A (5 μM) to determine background O_2 flux. These J_{O_2} values were subtracted from all prior measures to account for any artifactual non-ETS O_2 consumption (means ± SD across all experiments: 3.86 ± 1.39 pmol·s^{-1}·mg wet wt^{-1}). Measurements of oxygen fluxes were averaged from both chambers during steady state for each respiratory state. If one of the chambers did not reach steady-state flux, that value was excluded from the analysis of that respiratory state. Throughout the respiration protocol, rates of H_2O_2 emission were simultaneously assessed via the Amplex UltraRed (25 μM; Molecular Probes, Invitrogen) and horseradish peroxidase (2.5 U/ml) reaction with H_2O_2 in the presence of added SOD (2.5 U/ml). The formation of the fluorescent reaction product (resorufin) was measured via excitation/emission at 525/600 nm (Oroboros O2k-Fluorescence LED-2 Module; Anton Paar, Graz, Austria) (27, 34). Signal was calibrated at the beginning of each experiment with 40 nM titrations of H_2O_2 and expressed relative to sample mass (in mg/wet wt).

Real-time quantitative polymerase chain reaction. RNA was isolated from BASE and 3HR muscle samples by mechanical homogenization (Tissuelyser; Qiagen) with Tri reagent, followed by 1-bromo-3-chloropropane and isopropanol precipitation (Sigma-Aldrich, Castle Hill, NSW, Australia), which was then dissolved in DNase and RNase free water. RNA samples were tested spectrophotometrically (BioPhotometer, Eppendorf) for concentration at 260 nm and quality, indicated by the 260:288 nm absorbance ratio (means ± SD: 2.15 ± 0.18). One microgram of RNA was then reverse transcribed to cDNA (iScript kit; Bio-Rad, Gladesville, NSW, Australia). Real-time quantitative PCR reactions were carried out in a Mastercycler RealPlex 2 (Eppendorf, Hamburg, Germany) with Taq enzyme reagent (iTaq SYBR Green; Bio-Rad) and forward and reverse primers (Sigma-Aldrich) for target mRNAs, which were generated from the National Center for Biotechnology Information Primer-BLAST database as shown in Table 1. The conditions for RT-qPCR were an initial 3 min annealing phase at 95°C and then 40 cycles of 15 s at 95°C and 1 min at 60°C. After this, a 20-min melting curve (60°C to 95°C) was performed to confirm the amplification of a single product. Cycle thresholds (C_T) were calculated using software (RealPlex; Eppendorf) and used to quantify mRNA expression via the $-2\Delta\Delta C_T$ method (39) normalized to a housekeeping gene, β2 microglobulin (*β-2M*).

Muscle protein extraction and Western blotting. Frozen muscle was processed for Western blotting as per our previous work (66). Protein (6–8 μg per lane) was then loaded into precast 26-well stain-free 4–20% gradient gels (Criterion TGX Stain-Free Precast; Bio-Rad) along with molecular weight ladder (PageRuler Plus; Thermo Scientific) and pooled sample. The pooled sample was made by combining small volumes of all samples into a single pooled sample and used to construct a five-point standard curve (2 to 16 μg protein) on all gels to allow direct comparison of blot intensities via linear regression, as described in detail elsewhere (47). Stain-free gels were activated by UV light (ChemiDoc MP; Bio-Rad) and imaged to visualize the total protein of each lane. Proteins were then transferred to PVDF membranes (Trans-Blot Turbo; Bio-Rad), blocked, and then incubated overnight at 4°C with the following primary antibodies diluted 1:1,000 in TBST containing 5% BSA and 0.1% sodium azide: anti-phospho-acetyl CoA carboxylase (p-ACCβ^{Ser221}; no. 11818; Cell Signaling), anti-phospho AMP-activated protein kinase (p-AMPK-

Table 1. *List of primer sequences for real-time PCR*

Gene	NCBI Ref Seq	Forward Primer 5′-3′	Reverse Primer 5′-3′
β-2M	NM_004048.2	TGCTGTCTCCATGTTTGATGTATCT	TCTCTGCTCCCCACCTCTAAGT
BNIP3	NM_004052.3	TGGACGGAGTAGCTCCAAGA	AAAGAGGAACTCCTTGGGGG
DRP1	NM_012062.4	CACCCGGAGACCTCTCATTC	CCCCATTCTTCTGCTTCCAC
GPX1	NM_000581.2	CGCCACCGCGCTTATGACCG	GCAGCACTGCAACTGCCAAGCAG
MFN2	NM_014874.3	CCCCCTTGTCTTTATGCTGATGTT	TTTTGGGAGAGGTGTTGCTTATTTC
NFE2L2	NM_006164.4	AAGTGACAAGATGGGCTGCT	TGGACCACTGTATGGGATCA
PPARGC1A	NM_013261.3	GGCAGAAGGCAATTGAAGAG	TCAAAACGGTCCCTCAGTTC
PRDX1	NM_001202431.1	CCCAACTTCAAAGCCACAGC	AAAGGCCCCTGAACGAGATG
SOD1	NM_000454.4	GGTCCTCACTTTAATCCTCTAT	CATCTTTGTCAGCAGTCACATT
SOD2	NM_001024465.1	CTGGACAAACCTCAGCCCTA	TGATGGCTTCCAGCAACTC
TXNRD1	NM_003330.3	AGCATGTCATGTGAGGACGG	AGAGTCTTGCAGGGCTTGTC
UCP3	NM_003356.3	CCACAGCCTTCTACAAGGGATTTA	ACGAACATCACCACGTTCCA

β-2M, β_2 microglobulin; *BNIP3*, BCL2/adenovirus E1B 19-kDa interacting protein 3; *DRP1*, dynamin 1-like protein; *GPX1*, glutathione peroxidase-1; *MFN2*, mitofusin-2; *NFE2L2*, nuclear factor erythroid 2-related factor 2; *PPARGC1A*, peroxisome proliferator-activated receptor-γ coactivator 1-α; *PRDX1*, peroxiredoxin-1; *SOD1*, cytosolic superoxide dismutase 1; *SOD2*, mitochondrial manganese superoxide dismutase; *TXNRD1*, thioredoxin reductase 1; *UCP3*, uncoupling protein-3, NCBI, National Center for Biotechnology Information.

^{Thr172}; no. 2531; Cell Signaling), anti-dynamin-related protein 1 (DRP1; no. 5391; Cell Signaling), anti-glutathione (no. 19534; Abcam), anti-glutathione peroxidase 1 (GPX1; no. 3286; Cell Signaling), anti-phospho heat shock protein 27 (p-HSP27^{ser82}; ADI-SPA-524; Enzo), anti-heat shock protein 72 (HSP72 ADI-SPA-810; Enzo), Mitoprofile cocktail (no. MS601; MitoSciences consisting of anti-complex I subunit NDUFB8 (complex I; no. 110242; Abcam), anti-complex II subunit 30 kDa (complex I; no. 14714; Abcam), anti-complex III subunit core 2 (no. 14745; complex III; Abcam), anti-complex IV subunit II (complex IVs2; no. 110258; Abcam), anti-ATP synthase subunit-α (complex V; no. 14748; Abcam), anti-complex IV subunit IV (complex IVs4; no. MS407; Mito Sciences), anti-mitofusin 2 (MFN2; no. 9482; Cell Signaling), PRDX pathway cocktail [no. 184868; Abcam; consisting of anti-peroxiredoxin 1 (PRDX1), anti-thioredoxin (TRX), and anti-thioredoxin reductase-1 (TXNRD1)], anti-PPARγ coactivator-1α (PGC1α; no. 2178; Cell Signaling), anti-mitochondrial transcription factor 1 (TFAM; no. 475017; Abcam), and anti-uncoupling protein 3 (UCP3; no. 10985; Abcam). Membranes were then probed with appropriate horseradish peroxidase-conjugated secondary antibody (PerkinElmer, Glen Waverly, VIC, Australia), at a dilution of 1:50,000–100,000 in 5% nonfat milk TBST for 1 h at room temperature. ECL (SuperSignal West Femto; Thermo Scientific) was applied for imaging with a high-sensitivity CCD camera (ChemiDoc MP; Bio-Rad), and subsequent analysis was performed (ImageLab v 5.1; Bio-Rad). Total protein loading of each sample was determined from stain-free images of each gel, and these values were then used to normalize each protein of interest after normalization to its standard curve.

Coimmunoprecipitation of glutathionylated proteins. Frozen muscle was sectioned and homogenized as described above but with 200 μl nondenaturing lysis buffer [20 mM Tris·HCl pH 8, 137 mM NaCl;, 1% Triton X-100, 2 mM EDTA, 1% vol/vol protease inhibitor cocktail (Sigma-Aldrich), and 25 mM *N*-ethylmalemide]. Muscle lysate (50 μg protein) was added to 100 μl washed protein-A Sepharose beads (GE Health/Amersham Biosciences), with 1 μl antiglutathione primary antibody (no. 19534; Abcam), which was incubated for 4 h at 4°C with rotation. Antigen-antibody-bead conjugates were centrifuged and supernatant discarded (supernatant was tested for efficacy of immunoprecipitation pull-down during optimization), followed by an additional three washes. Subsequently, 50 μl denaturing lysis buffer (125 mM Tris·HCl, 4% SDS, 10% glycerol, 10 mM EGTA, and 100 mM DTT) were added to the bead-protein-antibody conjugate and then heated at 95°C for 5 min to elute proteins from the bead-antibody conjugate. Bromophenol blue dye (1% vol/vol) was added before SDS-PAGE and immunoblotting were performed as described above with the Mitoprofile cocktail (no. MS601; MitoSciences) and UCP3 (no. 10985; Abcam) antibodies.

Statistical Analysis

Data were analyzed by one-way (exercise-intensity) or two-way (exercise-intensity × time) ANOVA with repeated measures where appropriate (SPSS Statistics, IBM v1.0.0.642). Mauchly's test of sphericity was performed, and Greenhouse-Geisser correction was applied where nonsphericity was detected. Where significant main interaction, time, or exercise-intensity effects were detected, post hoc analyses were conducted with Bonferroni correction for multiple comparisons. Statistical significance was accepted at $P < 0.05$, and trends indicated at $P \leq 0.10$. Where significant main effects were detected, effect sizes (ES) were calculated on data pooled from all three exercise protocols for pairwise comparison between time points using Cohen's *d* with 95% lower to upper confidence intervals (CI), without correction for multiple comparisons. Data are reported as means ± SD for $n = 8$ unless otherwise stated.

RESULTS

Physiological Responses to Exercise

Total external work of work-matched CMIE and HIIE was fourfold greater than SIE (Table 2). Greater exercise intensity increased rating of perceived exertion (SIE > HIIE > CMIE, $P < 0.001$), despite HIIE leading to the highest peak heart rate ($P < 0.001$, Table 2).

Mitochondrial Respiration

State 4 leak respiration supported by complex I ($LEAK_{CI}$) or I + II ($LEAK_{CI + II}$) substrates was not differentially affected by exercise intensity but increased with time by 65% ($P = 0.003$; ES: 1.34; 95% CI: 1.03 to 1.65; Fig. 1*B*) and 40% ($P < 0.001$; ES: 0.77; 95% CI: 0.59 to 0.95; Fig. 1*C*), respectively, in a BASE versus EX comparison across all exercise protocols. At 3HR, $LEAK_{CI}$ remained ~30% elevated above BASE ($P < 0.047$; ES: 0.57; 95% CI: 0.33 to 0.82). State 3 oxidative phosphorylation (5 mM ADP) supported by complex I + II ($OXPHOS_{CI + II}$) was not affected by exercise intensity (exercise intensity × time, $P = 0.154$) but was ~15% lower at 3HR compared with EX across all exercise protocols ($P = 0.003$; ES: −0.27; 95% CI: −0.44 to −0.10; Fig. 1*D*). Uncoupled respiration (with FCCP) supported by complex I + II ($ETS_{CI + II}$) or II only (plus rotenone) was not affected by exercise intensity but was 15% ($P = 0.009$; ES −0.35; 95% CI: −0.53 to −0.16; Fig. 1*E*) and 30% ($P = 0.024$; ES: −0.52; 95% CI: −0.81 to −0.24; Fig. 1*F*) lower, respectively, at 3HR compared with EX across all exercise protocols. The J_{O_2} ratio between 0.25 vs. 5 mm ADP under $OXPHOS_{CI + II}$ conditions was not significantly affected by exercise protocol or time (data not shown).

Mitochondrial H_2O_2 Emission

During both complex I ($LEAK_{CI}$) and I + II ($LEAK_{CI + II}$) supported leak respiration, $J_{H_2O_2}$ was not affected by exercise intensity but was elevated ~55% during $LEAK_{CI}$ at 3HR relative to EX across all exercise protocols ($P = 0.018$; ES: 0.94; 95% CI: 0.55 to 1.33; Fig. 2*B*). In contrast, during $LEAK_{CI + II}$, $J_{H_2O_2}$ was ~30% lower at EX ($P = 0.008$; ES: −0.83; 95% CI: −1.08 to −0.57) and ~40% lower at 3HR ($P < 0.001$; ES: −0.97; 95% CI: −1.22 to −0.72; Fig. 2*C*)

Table 2. *Physiological demands and responses to acute exercise protocols*

	CMIE	HIIE	SIE
Total exercise session time includes rest periods, min	30 ± 0^{b,c}	24 ± 0^{a,c}	15 ± 0^{a,b}
Exercise time, min	30 ± 0^{b,c}	20 ± 0^{a,c}	2 ± 0^{a,b}
Mean power output, W	163 ± 36^{b,c}	245 ± 54^{a,c}	645 ± 71^{a,b}
Total mechanical work, kJ	294 ± 65^{c}	294 ± 65^{c}	76 ± 14^{a,b}
Intensity, %peak power output	50 ± 0^{b,c}	75 ± 0^{a,c}	198 ± 25^{a,b}
Intensity, $\%VO_{2peak}$	54 ± 3^{b,c}	77 ± 1^{a,c}	
HR, session peak, beats/min	158 ± 15^{b}	182 ± 11^{a,c}	168 ± 9^{b}
RPE, session peak, arbitrary units	13 ± 2^{b,c}	18 ± 1^{a,c}	20 ± 0^{a,b}

Data are means ± SD; $n = 8$. CMIE, continuous moderate-intensity exercise; HIIE, high-intensity interval exercise; SIE, sprint interval exercise; HR, heart rate; RPE, rating of perceived exertion (6–20). $^{a}P < 0.05$, compared with CMIE; $^{b}P < 0.05$, compared with HIIE; $^{c}P < 0.05$, compared with SIE.

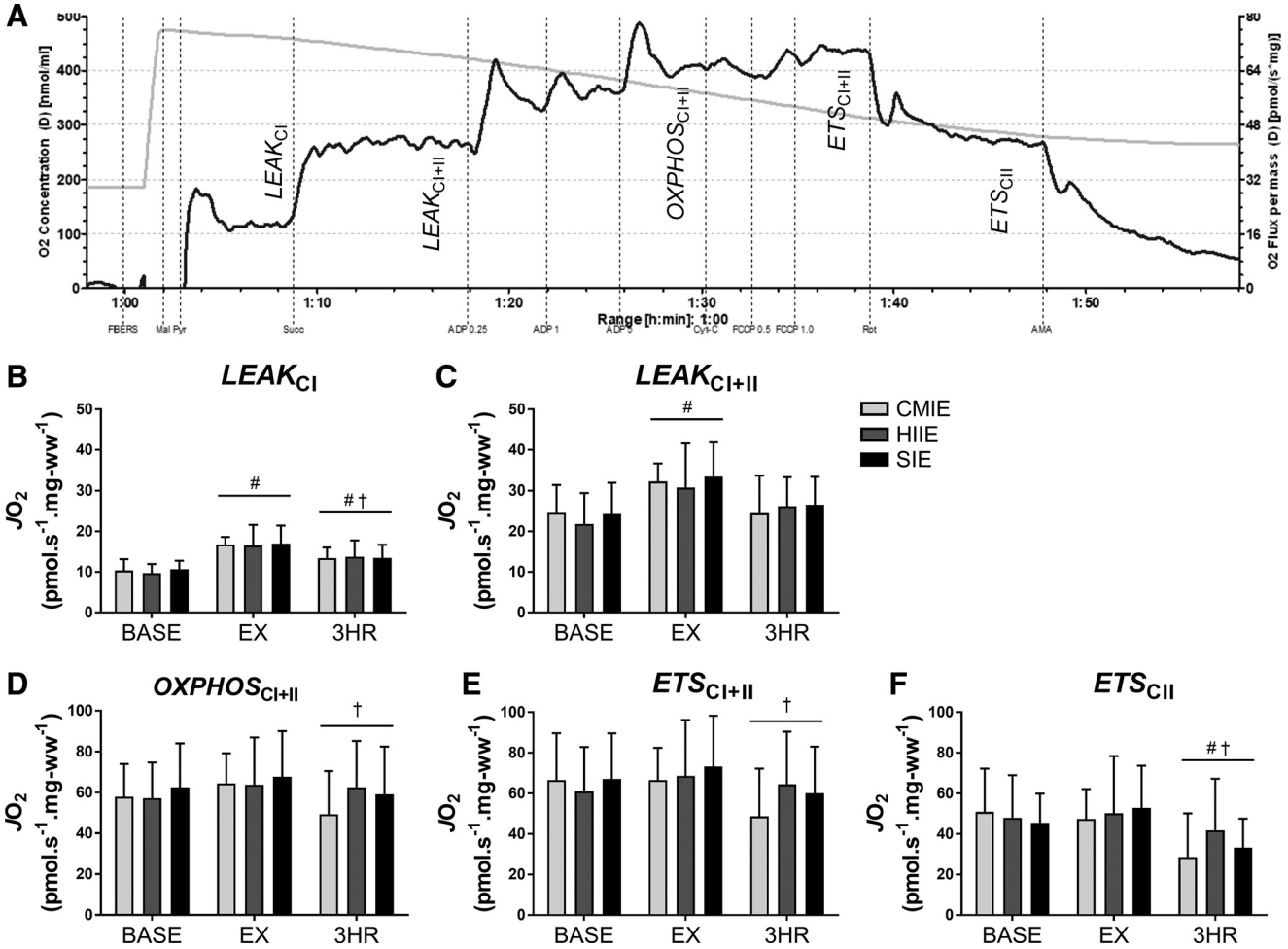

Fig. 1. Mitochondrial respiration from permeabilized human skeletal muscle fibers. *A*: representative mitochondrial oxygen flux (J_{O_2}) trace depicts 1 sample in a single chamber from a baseline condition. Light gray line (left *y*-axis) is chamber O_2 concentration, and dark line (right *y*-axis) is mitochondrial O_2 consumption (J_{O_2}) rate throughout the substrate inhibitor uncoupled titration protocol. *B–F*: various respiratory states were induced as follows: state 4 leak (*LEAK*) supported by complex I substrates malate and pyruvate (*B*), addition of succinate for complex II (*C*), ADP (5 mM)-stimulated state 3 (*OXPHOS*) (*D*), and uncoupled (*ETS*) states with complexes I + II (*E*) substrate input or complex II (*F*) only after rotenone complex I inhibition. Muscle samples were taken at baseline (BASE), immediately after exercise (EX), and after 3-h recovery (3HR). CMIE, continuous moderate-intensity exercise; HIIE, high-intensity interval exercise; SIE, sprint interval exercise; ww, wet weight muscle. Data are means ± SD; $n = 8$. Main time effect: #$P < 0.05$, compared with BASE, †$P < 0.05$, compared with EX.

relative to BASE across all exercise protocols. During complex I + II supported state 3 oxidative phosphorylation respiration ($OXPHOS_{CI+II}$), $J_{H_2O_2}$ was unaffected by exercise intensity but tended to be elevated ~65% at 3HR relative to EX across all protocols ($P = 0.057$; ES: 0.71; 95% CI: 0.32 to 1.10; Fig. 2*D*). Similarly, during uncoupled respiration (plus FCCP) supported by complex I + II substrates (ETS_{CI+II}), there was no effect of exercise intensity on $J_{H_2O_2}$ but this tended to be increased by ~95% ($P = 0.072$; ES: 0.63; 95% CI: 0.26 to 0.99; Fig. 2*E*) at 3HR compared with EX across all protocols. However, $J_{H_2O_2}$ was unaffected by exercise during uncoupled respiration supported by complex II only (plus rotenone; Fig. 2*F*). Expressed as a ratio relative to J_{O_2}, $J_{H_2O_2}$ was lower in $LEAK_{CI}$ at EX versus BASE ($P = 0.030$; ES: 1.01; 95% CI: −1.47 to −0.54), but during all other respiratory states the overall effects of exercise on this ratio closely reflected absolute $J_{H_2O_2}$ rates.

Protein Phosphorylation Responses to Exercise

There were no effects of exercise intensity on phosphorylation of $AMPK^{Thr172}$ ($P = 0.197$), $ACC\beta^{Ser221}$ ($P = 0.490$), or $HSP27^{Ser82}$ ($P = 0.568$); however, each of these increased by ~1.5-fold ($P = 0.001$; ES: 0.86; 95% CI: 0.52 to 1.19; Fig. 3*B*), ~2.5-fold ($P < 0.001$; ES: 2.15; 95% CI: 1.68 to 2.62; Fig. 3*C*), and ~2.5-fold ($P = 0.051$; ES: 1.09; 95% CI: 0.62 to 1.57; Fig. 3*D*) across all exercise protocols at EX relative to BASE, respectively.

Exercise and Redox-Sensitive Gene Expression

There were no significant effects of exercise intensity; however, there were main effects for increased skeletal muscle mRNA levels of *PPARGC1A* ($P = 0.027$; ES: 0.86; 95% CI: 0.47 to 1.25), *UCP3* ($P = 0.027$; ES:0.70; 95% CI: 0.31 to 1.09), *BNIP3* ($P = 0.010$; ES: 0.48; 95% CI: 0.09 to 0.88), and *PRDX1* ($P = 0.034$; ES: 0.36; 95% CI: −0.12 to 0.83) at 3HR

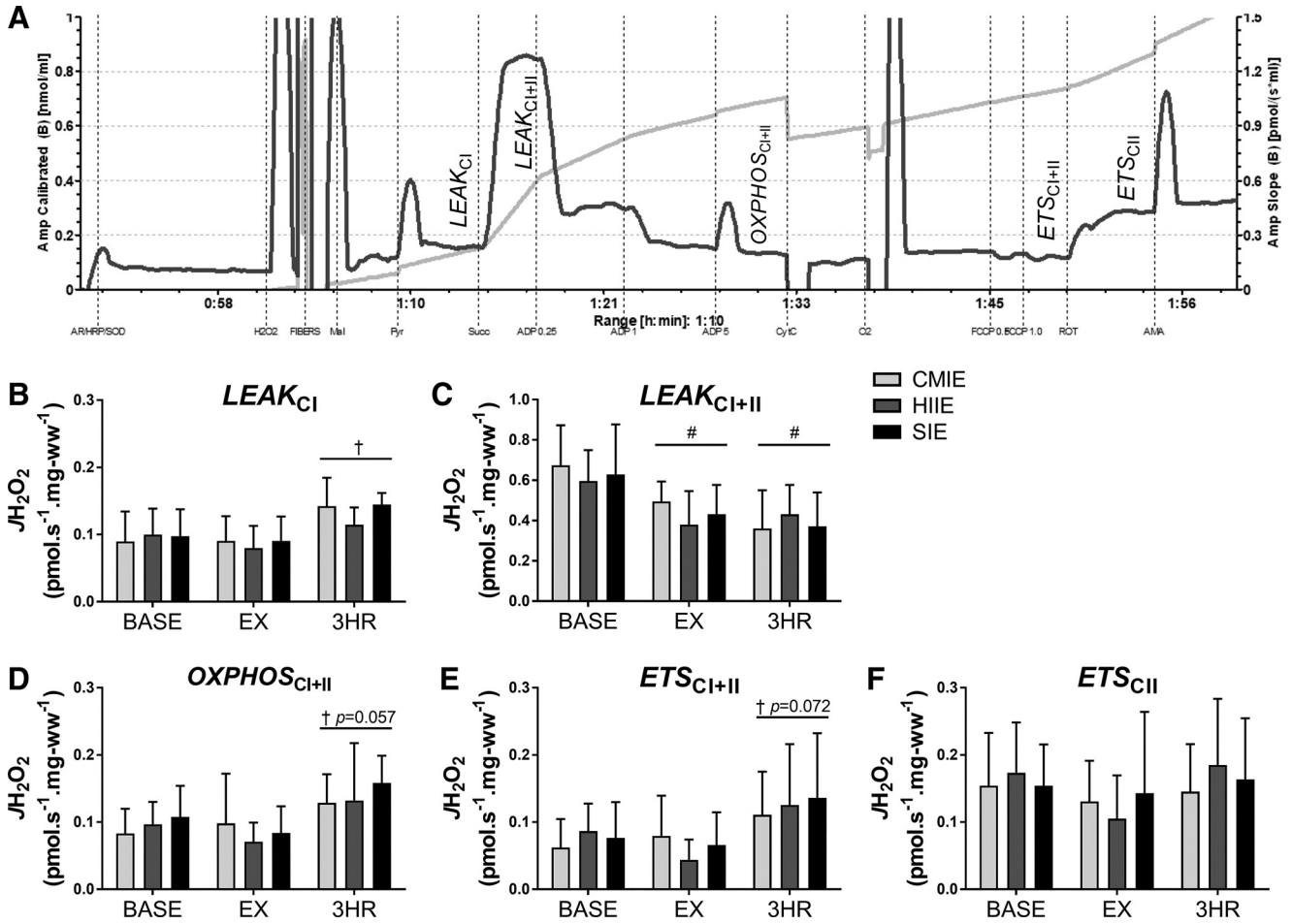

Fig. 2. Mitochondrial H_2O_2 emission from permeabilized human muscle fibers. *A*: representative mitochondrial hydrogen peroxide trace depicts 1 sample in a single chamber from a baseline condition. *B–F*: light gray line (left *y*-axis) is cumulative Amplex UltraRed fluorescent reaction product in the chamber proportional to H_2O_2 formation, dark line (right *y*-axis) is H_2O_2 emission rate ($J_{H_2O_2}$) throughout the substrate inhibitor uncoupled titration protocol used to induce various respiratory states: state 4 leak (*LEAK*) supported by complex I substrates malate and pyruvate (*B*), addition of succinate for complex II (*C*), ADP (5 mM) stimulated state 3 (*OXPHOS*) (*D*), and uncoupled (ETS) states with complexes I + II (*E*) substrate input or complex II (*F*) only after rotenone complex I inhibition. Muscle samples were taken at baseline (BASE), immediately after exercise (EX), and after 3-h recovery (3HR). CMIE, continuous moderate-intensity exercise; HIIE, high-intensity interval exercise; SIE, sprint interval exercise; ww, wet weight muscle. Data are means ± SD; $n = 8$. Main time effect unless otherwise stated: #$P < 0.05$, compared with BASE, †$P < 0.05$, compared with EX.

relative to BASE across all exercise protocols (Fig. 4, *A* and *B*). There were trends for increases in *MFN2* ($P = 0.057$; ES: 0.37; 95% CI: −0.03 to 0.76), *DRP1* ($P = 0.091$; ES: 0.45; 95% CI: 0.06 to 0.85), *GPX1* ($P = 0.092$; ES: 0.58; 95% CI: 0.19 to 0.98), and *TXNRD1* ($P = 0.069$; ES: 0.43; 95% CI: 0.04 to 0.82) mRNA levels at 3HR compared with BASE across all protocols, while there were no main effects of time on *NFE2L2* ($P = 0.427$) or *SOD1* ($P = 0.282$) or *SOD2* mRNA ($P = 0.186$; Fig. 4*B*).

Skeletal Muscle Antioxidant and Mitochondrial Protein Abundance

Overall, we found no effect of time nor exercise intensity in the expression levels of key antioxidant enzymes TRX and GPX1; the chaperone HSP72; mitochondria-related proteins MFN2, DRP1, and PGC1α (Fig. 5); or complexes I–V (Fig. 6). However, there was significantly decreased abundance of PRDX1 by approximately −35% ($P = 0.033$; ES: −0.69; 95% CI: −0.95 to −0.44; Fig. 5*B*), TFAM by ~15% ($P = 0.007$; ES: −0.34; 95% CI: −0.54 to −0.14; Fig. 5*J*) and a tendency for lower UCP3 by ~20% ($P = 0.078$; ES: −0.56; 95% CI: −0.82 to −0.30; Fig. 5*I*) at 3HR compared with BASE across all exercise protocols. There was a significant main interaction effect of exercise intensity × time on thioredoxin reductase (TXNRD1) protein abundance ($P = 0.032$). Specifically, at EX, there was ~35% less TXNRD1 protein detected following the CMIE protocol compared with the SIE protocol ($P = 0.007$; ES: −0.72; 95% CI: −1.33 to −0.10; Fig. 5*E*).

Mitochondrial Protein S-Glutathionylation

No significant effects of exercise were found for *S*-glutathionylation of mitochondrial proteins ATP-synthase-α ($P = 0.975$), complex $IV^{subunit2}$ ($P = 0.931$), or UCP3 ($P = 0.668$; Fig. 7).

DISCUSSION

The present study design allowed for a direct within-subject comparison of mitochondrial responses to acute bouts of CMIE and HIIE on a work-matched basis, as well as comparisons of

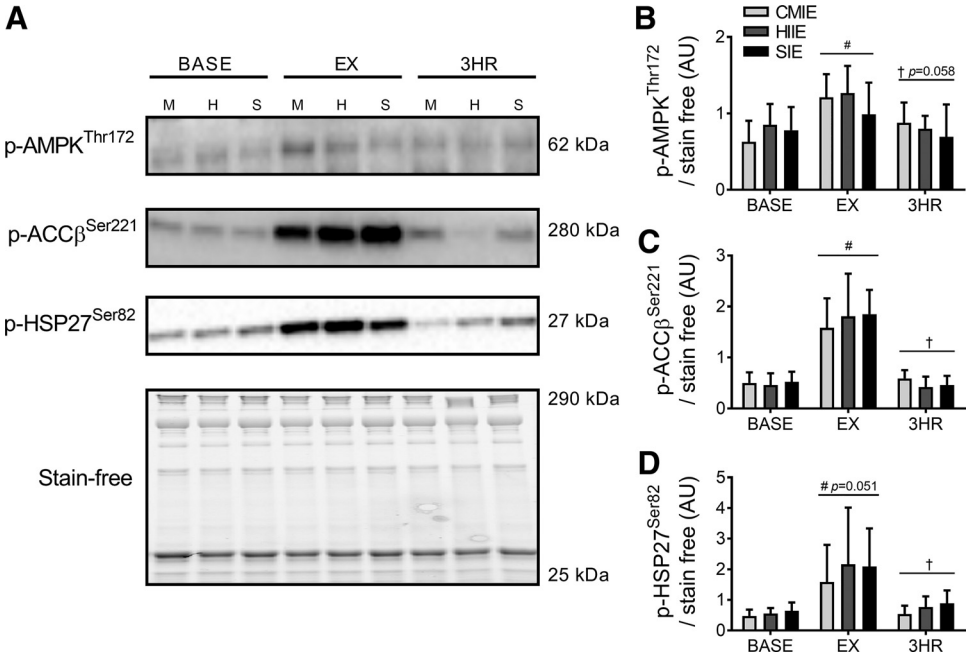

Fig. 3. Muscle protein phosphorylation responses to exercise. *A*: representative Western blots. *B–D*: blots were quantified for AMP-activated protein kinase at threonine 172 (*C*), phosphorylated acetyl-coA carboxylase at serine 221 (*B*), and heat shock protein of 27-kDa serine 82 (*D*) before (BASE), immediately (EX), and 3 h (3HR) after continuous moderate-intensity (CMIE), high-intensity interval (HIIE), and sprint interval exercise (SIE); AU, arbitrary units. Representative blots are from a single participants' samples. Blot densitometry was normalized to stain-free total protein and quantified relative to standard curves generated on each membrane (not shown). Data are means ± SD; $n = 8$. Main time effect unless otherwise stated: #$P < 0.05$, compared with BASE, †$P < 0.05$, compared with EX.

these with low-volume sprint interval exercise (~25% of the total work volume of CMIE/HIIE) in young healthy humans. The main findings were that regardless of the exercise protocol performed, peak mitochondrial H_2O_2 emission (during nonphosphorylating complex I + II supported respiration) was lower immediately postexercise, yet rates of mitochondrial H_2O_2 emission tended to be elevated 3 h later during complex I + II supported ADP-stimulated oxidative phosphorylation and also uncoupled respiratory states. These acute changes in mitochondrial oxidant emission occurred concomitantly with increases in mitochondrial oxygen consumption rates during nonphosphorylating respiratory states immediately postexercise, yet 3 h postexercise oxygen consumption was lower during oxidative phosphorylation and uncoupled respiratory rates. Consistent with these acute mitochondrial responses to exercise, a range of key muscle metabolism-related protein phosphorylation events, as well as gene and protein expression of putative redox-sensitive targets, generally increased to equivalent levels in the early postexercise period regardless of protocol.

In the present study, higher exercise intensity had more pronounced effects on systemic physiological responses as indicated via session peak heart rate and rating of perceived exertion, in addition to blood lactate, glucose, and activity of specific stress-activated protein kinases, recently reported elsewhere (50, 51). Despite this, we found no exercise protocol-dependent effects on mitochondrial parameters. To establish where these divergent responses to different exercise protocols occurred (i.e., only at the mitochondria or also at the whole muscle level), we assessed key molecular markers of skeletal muscle energy metabolism and overall stress induced by the exercise protocols. Intriguingly, phosphorylation of AMPK-^{Thr172} (indicative of cellular bioenergetic perturbation) increased to a similar degree regardless of exercise protocol, as did its downstream substrate ACCβ^{Ser221}. Furthermore, mRNA expression of *PPARGC1A*, the gene encoding PGC1α and a target of AMPK signaling, increased ~13-fold at 3 h postexercise, regardless of exercise protocol. Previously, Egan et al. (18) reported that high-intensity continuous exercise generated greater mitochondrial biogenesis signaling than work-matched moderate-intensity continuous exercise. A possible explanation for this is the longer exercise duration and that the lowest exercise intensity protocol employed in that study (18) was 40% $\dot{V}O_{2peak}$, whereas the lowest in the present study was ~55% $\dot{V}O_{2peak}$. Indeed, the 3 h postexercise increases in *PPARGC1A* mRNA expression, p-AMPK, and p-ACC in all intensities of the present study are similar to what was reported for their HIIE (80% $\dot{V}O_{2peak}$) exercise. In support of this notion, Chen et al. (8) demonstrated that AMPK phosphorylation only occurred following exercise at 60% $\dot{V}O_{2peak}$ and above but not at 40% $\dot{V}O_{2peak}$. Recently, a well-designed study by MacInnis et al. (40) compared training responses to single-leg cycling CMIE in one leg and HIIE matched for both work and duration in the opposite leg. They reported superior mitochondrial adaptations (assessed via increased citrate synthase activity and mitochondrial respiratory rates) following HIIE training, although this occurred in a fiber-type-dependent manner (40), the effects of which are likely an important factor in the long-term response to training (38). It is possible that there were additional factors not controlled for in the present study that may contribute to a greater response to repeated bouts (i.e., training) of HIIE compared with CMIE, such as number of transitions between work and rest (10). Nevertheless, our findings are consistent with other studies comparing HIIE to CMIE that have reported equivalent, but not greater adaptive responses when matched for total work performed (3, 72). Interestingly, we also found that SIE led to equivalent mitochondrial and signaling responses as the CMIE and HIIE, despite consisting of considerably less total work. This suggests that the stimulus provided by each of the exercise protocols in the present study reached a threshold at least sufficient for activation of the assessed signaling pathways in muscle. Indeed, this is in line with earlier findings demonstrating the efficacy of low volume SIE (5, 22, 25). However, the

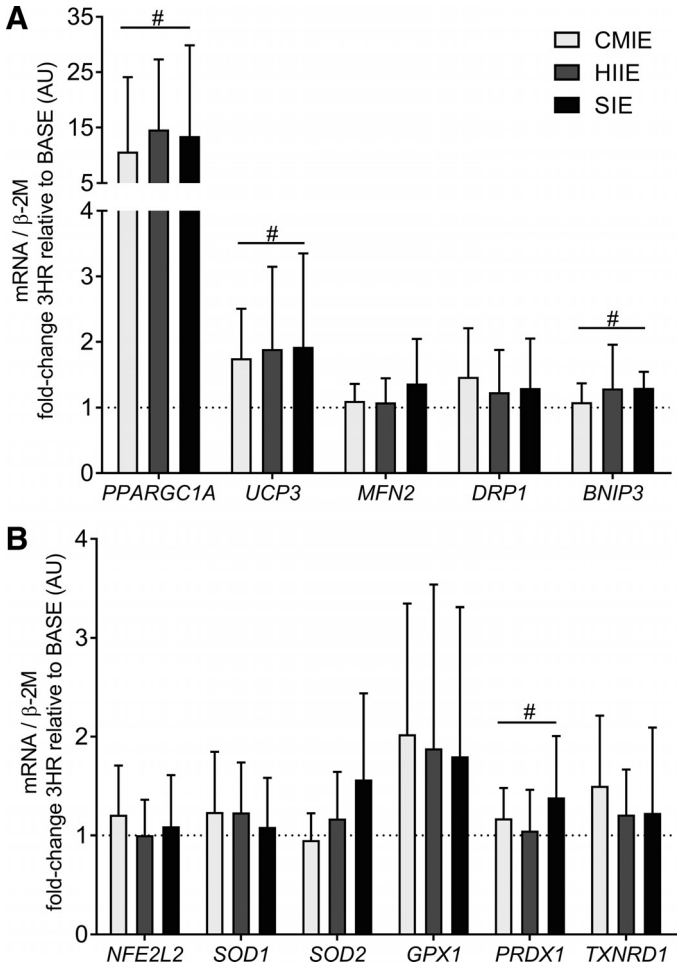

Fig. 4. *A* and *B*: mRNA expression of genes associated with mitochondrial biogenesis, morphology and mitophagy (*A*) and redox homeostasis (*B*) 3 h after the different exercise bouts. Muscle mRNA expression analyzed by quantitative PCR is fold-change normalized to a housekeeping gene, β2-microglobulin (β-2M) at 3 h postexercise relative to respective baseline (depicted by dashed line). CMIE, continuous moderate-intensity exercise; HIIE, high-intensity interval exercise; SIE, sprint interval exercise; AU, arbitrary units. Data are means ± SD; $n = 8$. Main time effect across all exercise protocols: #$P < 0.05$, compared with baseline. *BNIP3*, BCL2/adenovirus E1B 19-kDa interacting protein 3; *DRP1*, dynamin 1-like protein; *GPX1*, glutathione peroxidase-1; *MFN2*, mitofusin-2; *NFE2L2*, nuclear factor erythroid 2-related factor 2; *PPARGC1A*, peroxisome proliferator-activated receptor-γ coactivator 1-α; *PRDX1*, peroxiredoxin-1; *SOD1*, cytosolic superoxide dismutase 1; *SOD2*, mitochondrial manganese superoxide dismutase; *TXNRD1*, thioredoxin reductase 1; *UCP3*, uncoupling protein-3.

complexity of the molecular signals generated and transduced in response to exercise should not be understated, since other signaling pathways can be differentially activated to ultimately elicit specific training adaptations to distinct exercise modalities (51). Taken together, our findings nevertheless support the notion that similarly robust molecular signals can be generated in skeletal muscle in response to a broad range of exercise stimuli.

Relatively few studies have investigated acute postexercise changes in mitochondrial function. Given that $O_2^{\cdot-}/H_2O_2$ generation is intrinsically linked to the respiratory state (11), the present findings of altered mitochondrial H_2O_2 emission in the hours postexercise in a respiratory state-dependent manner are consistent with previous reports from our group and others showing that exercise acutely alters mitochondrial respiration (37, 63, 64, 66). Despite the lack of effect of exercise intensity, there was a robust and dynamic effect of acute exercise on mitochondrial function, such as decreasing postexercise $J_{H_2O_2}$ during the succinate driven $LEAK_{CI+II}$ respiration state. Succinate-driven $J_{H_2O_2}$ formation occurs primarily via superoxide generation due to reverse electron flow through the flavin mononucleotide site in complex I under experimental conditions of high inner mitochondrial membrane potential in the absence of ADP (46). Conceivably, high membrane potential could occur during situations of prolonged low ATP demand (24) such as with physical inactivity and sedentary lifestyle. Our findings therefore suggest a mechanism by which exercise may decrease $J_{H_2O_2}$ in the postexercise "basal" respiratory state. This may be pertinent for attenuation of oxidative stress that has been associated with various pathophysiological states including insulin resistance (32).

The decreased postexercise H_2O_2 emission under reverse electron flow mitochondrial respiratory conditions may be attributed to increased proton leak (i.e., uncoupling) at the inner mitochondrial membrane in response to exercise. This is supported by our finding of simultaneously increased postexercise O_2 flux under the same $LEAK_{CI+II}$ respiratory state and is consistent with findings from an earlier study using permeabilized muscle mitochondria in young, healthy humans (63). The increased postexercise mitochondrial membrane proton leak would also decrease proton-motive force available to drive ATP synthesis. This supports our observation of lower state 3 ADP stimulated oxidative-phosphorylation (*OXPHOS*) respiration at 3 h postexercise and is comparable to the changes observed in permeabilized muscle mitochondria following high-intensity running in horses (69). One previous study in humans reported no change in *OXPHOS* J_{O_2} following exhaustive human exercise (64). However, their measurements were made under conditions where the flux of substrates through the ETS would be submaximal, since only complex I substrates were used with no convergent electron input from the complex II substrate succinate, likely masking any effect of exercise on maximal *OXPHOS* activity. It should be noted, however, that we cannot exclude the potential contribution of pyruvate dehydrogenase activity, which is well known to be regulated by exercise (54). Given that we used pyruvate as the sole complex I substrate, this may affect substrate availability for complex I in our experimental system. Nevertheless, during this $OXPHOS_{CI+II}$ respiratory state, we found a trend for elevated $J_{H_2O_2}$ at 3 h postexercise and a significant elevation with uncoupled ETS_{CI+II}. This is despite the ETS functioning in the "normal" forward direction under these respiratory states (i.e., any $O_2^{\cdot-}/H_2O_2$ formed not via reverse electron flow). This suggests that the elevated $O_2^{\cdot-}/H_2O_2$ formed specifically in this ADP stimulated state 3 respiratory state may be attributed to altered ETS respiratory complex activity, potentially via exercise-induced posttranslational modifications. Intriguingly, the trend for elevated $J_{H_2O_2}$ at 3 h postexercise during uncoupled respiration was absent after the addition of rotenone (ETS_{CII}), suggesting an effect of exercise directly or indirectly at the complex I_Q site (74). While it should be noted that the use of inhibitors and saturating substrate concentrations used in our ex vivo preparation may not recapitulate the native in vivo cellular environment and rates of superoxide formation, these findings nonetheless highlight that

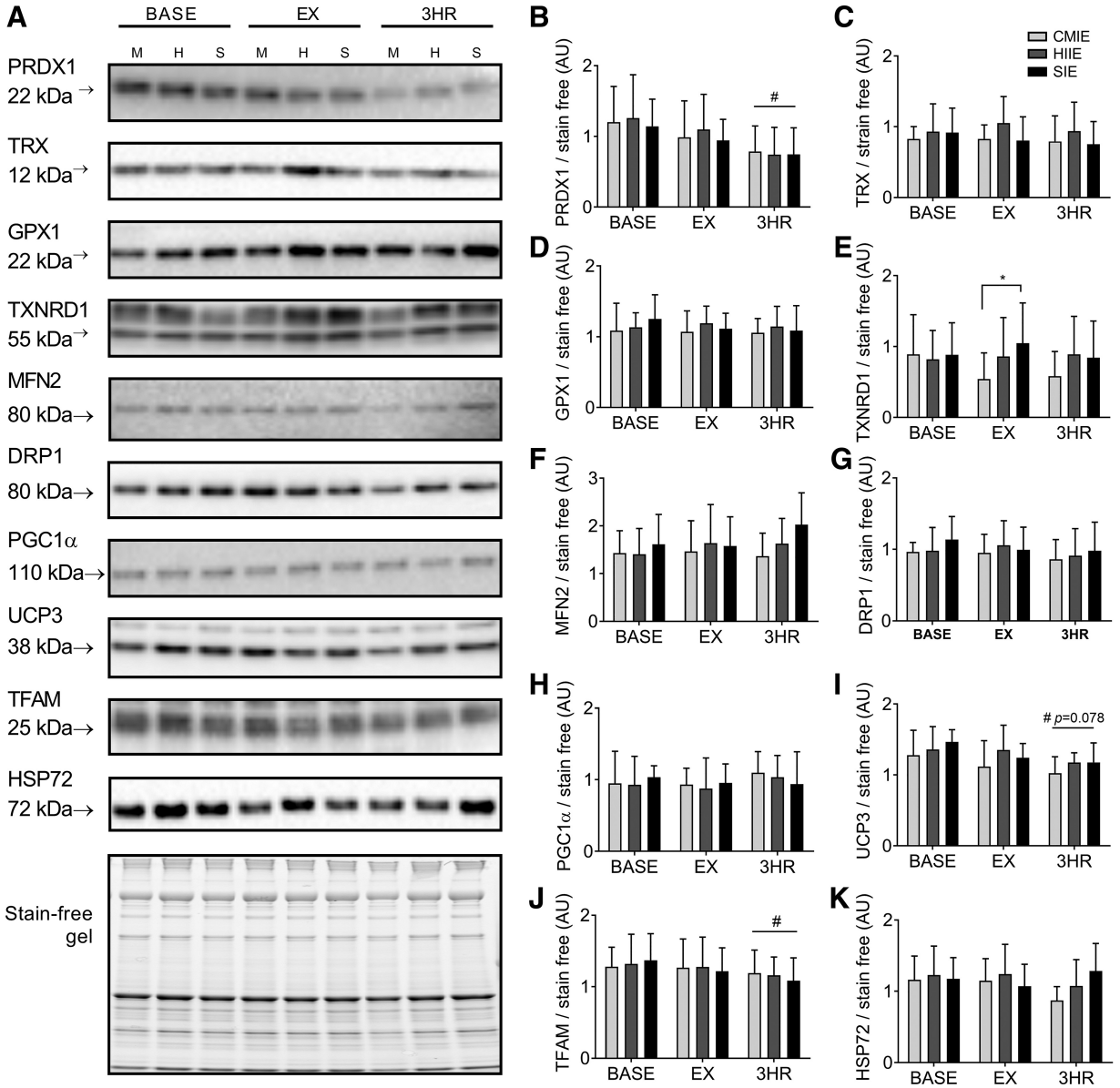

Fig. 5. Proteins involved in redox homeostasis and mitochondrial function. *A*: representative Western blots. *B–K*: blots were quantified for antioxidant proteins peroxiredoxin (PRDX1; *B*), thioredoxin (TRX; *C*), glutathione peroxidase-1 (GPX1; *D*), and thioredoxin reductase-1 (TXNRD1; *E*); mitochondrial morphology proteins mitofusin-2 (MFN2; *F*) and dynamin-related protein-1 (DRP1; *G*); mitochondrial proteins peroxisome proliferator-activated receptor-γ coactivator 1-α (PGC1α; *H*), uncoupling protein 3 (UCP3; *I*), and mitochondrial transcription factor A (TFAM; *J*); and heat-shock protein of 72 kDa (HSP72; *K*). Blot densitometry was normalized to stain-free total protein and quantified relative to internal calibration curves on each membrane. Exercise was continuous moderate-intensity (CMIE), high-intensity interval (HIIE), and sprint interval (SIE) exercise samples obtained at baseline (BASE), immediately postexercise (EX), and after 3-h recovery (3HR); AU, arbitrary units. Representative blots are shown from 1 subject. Data are means ± SD; $n = 8$. Main time effect unless otherwise stated: #$P < 0.05$, compared with BASE. *$P < 0.05$ exercise intensity effect.

acute exercise can modify *1*) mitochondrial inner membrane proton leak, and *2*) ETS-derived $O_2^{\cdot-}/H_2O_2$ emission characteristics in the hours postexercise.

Mitochondrial function may be regulated by redox-mediated posttranslational modifications such as *S*-glutathionylation of cysteine residues within ETS proteins (42). To investigate this possibility in the context of exercise, we probed *S*-glutathionylation of mitochondrial ETS subunits including ATP-synthase subunit-α (complex V) and cytochrome *c* oxidase subunit 2 (complex IV) using the mitochondrial cocktail antibody following immunoprecipitation with anti-GSH (Fig. 7). We were unable to observe any significant effects of exercise on these, possibly as a result of limited sample material only allowing for $n = 4$. While the NDUFB8 complex I subunit detected by the commonly used mitochondrial cocktail antibody did not display detectable levels of *S*-glutathionylation, other subunits of complex I such as NDUFS7 and NDUFV1 contain iron-sulfur clusters susceptible to oxidation and are known regulators of complex I $O_2^{\cdot-}/H_2O_2$ generation (17, 23). We also probed for *S*-glutathionylation of UCP3, which is known to regulate inner mitochondrial membrane potential and thereby modulate respiratory function and rates of superoxide formation (43). Although we also did not detect significant effects of exercise on this, future studies may

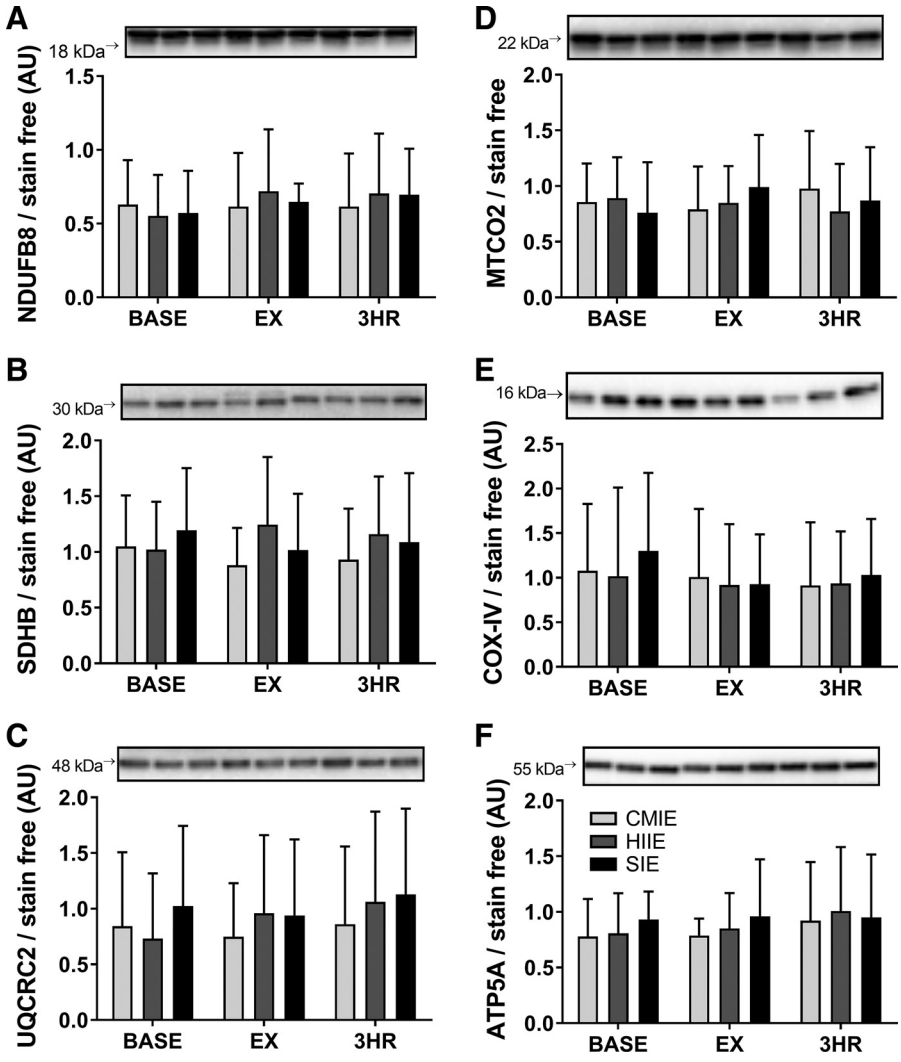

Fig. 6. Mitochondrial complex I–V protein abundance. *A–F*: subunits of complex I (NDUFB8) (*A*), II (SDHB) (*B*), III (UQRCR2) (*C*), IV subunit 2 (MTCO2) (*D*), IV subunit 4 (COX-IV) (*E*), and V (ATP5A) (*F*) were assessed by Western blot. Exercise was continuous moderate-intensity (CMIE), high-intensity interval (HIIE), and sprint interval (SIE) exercise samples obtained at baseline (BASE), immediately postexercise (EX), and after 3-h recovery (3HR); AU, arbitrary units. Blot densitometry was normalized to stain-free total protein, and quantified relative to internal calibration curves on each membrane. Representative blots are shown from 1 subject. Data are means ± SD; $n = 8$.

utilize mass spectrometry to investigate these and other redox-mediated posttranslational protein modifications in further detail (33).

We observed a decrease in PRDX1 protein abundance in muscle at 3 h postexercise, a cytosolic protein with low K_m for H_2O_2 (i.e., scavenges low levels of H_2O_2) (6). The decreased PRDX1 abundance at 3 h postexercise could impair the scavenging of mitochondrial H_2O_2, allowing localized ROS accumulation for the induction of redox signaling. This decrease is consistent with a recent report demonstrating that peroxiredoxins are rapidly degraded by ubiquitin mediated processes after being oxidized (59). Potentially in response to this, there was a small yet significant increase in *PRDX1* mRNA levels 3 h postexercise, supporting the notion that the PRDX/TRX antioxidant pathway plays an important role in exercise-induced redox signaling (70). TXNRD1 is a cytosolic protein that reduces TRX using NADPH, to in turn reduce PRDX. Interestingly, TXNRD1 protein content was lower after CMIE compared with SIE. This was the sole indication of a significant exercise protocol-dependent effect on muscle redox homeostasis in the present study. It is possible that similar mechanisms exist for the degradation of TXNRD1 similar to that of peroxiredoxins (59). We recently reported elsewhere that specific components of muscle and plasma redox homeostasis pathways were affected by exercise intensity (50). Therefore, it is tempting to speculate that different exercise protocols may exert subtle, yet important, effects in fine-tuning specific aspects of muscle redox homeostasis, which warrant further investigation.

The *NFE2L2* gene encodes NRF2, a redox-sensitive transcription factor and master-regulator of the antioxidant transcriptional response (15). Although *NFE2L2* mRNA was unchanged 3 h after exercise, it is likely that this would have peaked and returned to baseline levels before the 3-h postexercise time point (15, 48). Interestingly, downstream gene targets of NRF2 were not significantly affected by exercise: *SOD1*, *SOD2*, and *GPX1* mRNA expression, although there was a small yet significant increase in *PRDX1* mRNA at 3 h postexercise. It is possible that the exercise protocols in the present study, irrespective of work, were not sufficient for full activation of the NRF2 transcriptional response or at least at the time points assessed. Among other putative redox- and exercise-sensitive responses assessed, cytosolic heat-shock protein HSP27 phosphorylation increased postexercise as expected, while total abundance of the higher molecular weight HSP72 protein was unaffected. Previously, exercise intensity-

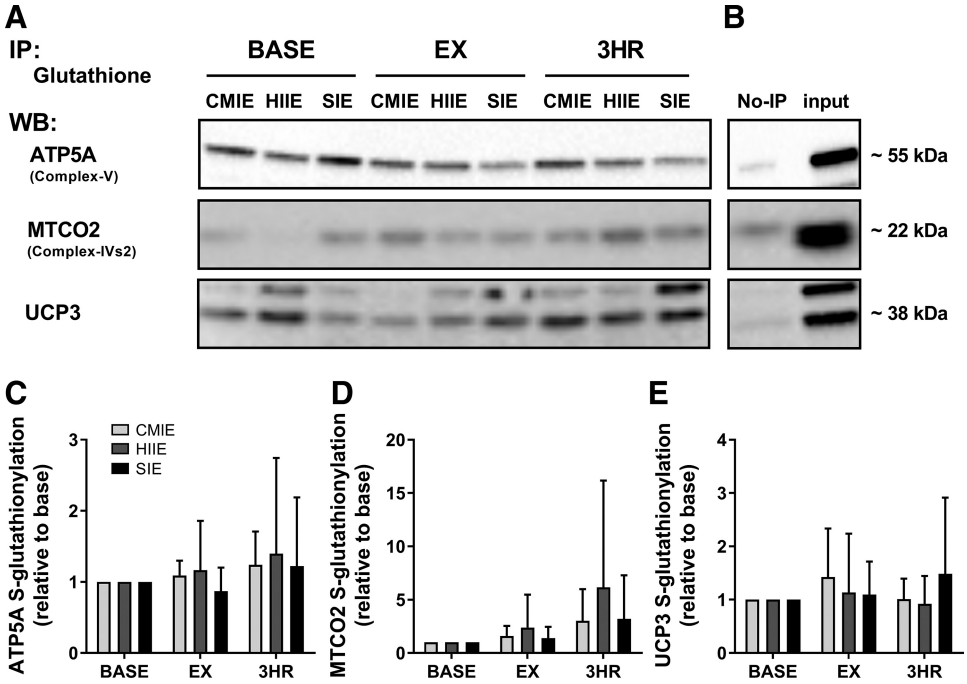

Fig. 7. Mitochondrial protein *S*-glutathionylation. Protein (50 μg) from whole muscle lysate was coimmunoprecipitated (co-IP) with anti-GSH antibody on sepharose beads then detected via Western blot (WB), as per METHODS. *A* and *B*: representative images show mitochondrial complexes V (ATP5A), IV subunit 2 (MTCO2), and uncoupling protein 3 (UCP3) from 1 subject at each time point (*A*) and co-IP pull-down was confirmed on the same membrane using a negative control in the absence of anti-GSH antibody in the pull-down (No-IP), along with whole muscle lysate as positive control (lysate) (*B*). *C–E*: protein *S*-glutathionylation was expressed relative to each respective baseline level of protein glutathionylation. Exercise was continuous moderate-intensity (CMIE), high-intensity interval (HIIE), and sprint interval (SIE) exercise, samples obtained at baseline (BASE), immediately postexercise (EX), and after 3-h recovery (3HR). Data are means ± SD; n = 3–4.

dependent increases of HSP72 were shown in rat skeletal muscle (44) as well as 3 days after HIIE in humans (9), and this has also been shown to occur via an exercise-induced $O_2^{\cdot-}$/H_2O_2 pathway (58). However, numerous environmental factors and molecular signals can also induce HSP72 expression in addition to $O_2^{\cdot-}$/H_2O_2 (14, 56). We observed an increase in *BNIP3* mRNA expression 3 h postexercise, which is involved in the mitochondrial quality control processes via mitophagy (75). Mitophagy has previously been shown to be affected by exercise via both PGC1α (68) and $O_2^{\cdot-}$/H_2O_2 (36). Our data suggest this response is not differentially affected by exercise intensity in human muscle, consistent with many of the other mitochondrial parameters measured in this study. Also unaffected by the present exercise protocols was abundance of DRP1 and MFN2, which regulate outer mitochondrial membrane fission and fusion, respectively. MFN2 protein levels did however show a tendency to increase to a greater extent at 3 h postexercise with SIE compared with CMIE. This is in line with previous literature showing that MFN2 protein was unchanged after 3 h of "low" intensity voluntary wheel running in mice (52) yet increased 3 h after 60 min of exercise at 70% $\dot{V}O_{2peak}$ in healthy middle-aged humans (35). Nevertheless, it should be noted that postexercise mitochondrial dynamics are most likely determined by acute posttranslational modifications to fission/fusion proteins rather than their total abundance alone (65).

While this randomized crossover study design provided a number of novel findings, some potential limitations should also be considered. The small sample size and sex distribution (male, n = 6; female, n = 2) in the present study preclude the detection of potentially subtle sex-dependent differences in responses to exercise (20). Although we tested females during the early follicular phase of the menstrual cycle to minimize the impact of ovarian hormone fluctuations and that skeletal muscle mitochondrial respiratory function was previously shown to be equivalent between men and women (61), sex-specific effects should nevertheless be considered in future investigations. Higher intensity exercise involves the recruitment of a greater proportion of fast twitch fibers (73); however, in the present study, fiber-type specific responses were not assessed, which could potentially mask some exercise-intensity specific effects as recently reported (40). In our mitochondrial respiration experiment, addition of succinate before ADP in the absence of rotenone stimulates maximal levels of superoxide production due to reverse electron transfer, and the effect of exercise on this was a key outcome measure in the present study. However, it should be acknowledged that the ROS generated in this respiratory state could influence subsequent respiratory measures by altering redox-sensitive components of the ETS or other proteins such as the adenine nucleotide translocase. Because of limited sample material, it was not possible to measure cellular glutathione levels (GSH and the oxidized form GSSG), which would have been informative to understand whether the observed postexercise changes in $J_{H_2O_2}$ were primarily due to altered rates of ROS generation alone or whether changes in GSH-mediated oxidant scavenging also contributed to this effect. It is also possible that other non-ETS mitochondrial enzymes not assessed in the present study could contribute to the background net emission of mitochondrial H_2O_2. Finally, it should be noted that while the Amplex UltraRed assay is intended to report mitochondrial H_2O_2 emission toward the cytosol, it may not be exclusive to this since the fluorescent reaction product resorufin has been shown to interact with intracellular sources of peroxides and/or peroxynitrites (13) or carboxylesterases (45). Thus it is conceivable that this could confound absolute quantification of $J_{H_2O_2}$ in the present study. However, the relative changes in $J_{H_2O_2}$ observed can be attributed to specific ETS sites, since these effects were observed only with their respective site-specific substrate and/or inhibitor combination.

Perspectives and Significance

In conclusion, we provide novel evidence that mitochondrial function (respiration and H_2O_2 emission) in human skeletal muscle are transiently altered in a respiratory state-dependent manner in the hours following continuous moderate- and high-intensity interval exercise irrespective of whether these exercise modes are matched for total work. Moreover, regardless of exercise protocol, there were comparable responses across a range of known and putative redox- and exercise-sensitive transcriptional and protein responses. Importantly, a total of only 2 min of sprint interval exercise was sufficient to elicit similar responses as 30 min of continuous moderate-intensity aerobic exercise. This suggests that exercise may be prescribed according to individual preferences while still generating similar signals known to confer beneficial metabolic adaptations. These findings have important implications for improving our understanding of how exercise can be used to enhance metabolic health in the general population.

ACKNOWLEDGMENTS

We are extremely grateful for the generous efforts of the volunteers who enthusiastically participated in this study.

Present address of A. J. Trewin: Dept. of Anesthesiology and Perioperative Medicine, Univ. of Rochester Medical Center, Rochester, NY.

GRANTS

N. K. Stepto was supported by the Australian Governments Collaborative Research Network. I. Levinger was supported by Future Leader Fellowship (ID: 100040) from the National Heart Foundation of Australia.

DISCLOSURES

No conflicts of interest, financial or otherwise, are declared by the authors.

AUTHOR CONTRIBUTIONS

A.J.T., C.S.S., I.L., G.K.M., and N.K.S. conceived and designed research; A.J.T., L.P., C.S.S., D.H., A.P.G., I.L., G.K.M., and N.K.S. performed experiments; A.J.T. analyzed data; A.J.T., L.P., C.S.S., D.H., I.L., G.K.M., and N.K.S. interpreted results of experiments; A.J.T. prepared figures; A.J.T. drafted manuscript; A.J.T., L.P., C.S.S., D.H., A.P.G., I.L., G.K.M., and N.K.S. edited and revised manuscript; A.J.T., L.P., C.S.S., D.H., A.P.G., I.L., G.K.M., and N.K.S. approved final version of manuscript.

REFERENCES

1. **Anderson EJ, Neufer PD.** Type II skeletal myofibers possess unique properties that potentiate mitochondrial H_2O_2 generation. *Am J Physiol Cell Physiol* 290: C844–C851, 2006. doi:10.1152/ajpcell.00402.2005.
2. **Archer SL.** Mitochondrial dynamics–mitochondrial fission and fusion in human diseases. *N Engl J Med* 369: 2236–2251, 2013. doi:10.1056/NEJMra1215233.
3. **Bartlett JD, Hwa Joo C, Jeong TS, Louhelainen J, Cochran AJ, Gibala MJ, Gregson W, Close GL, Drust B, Morton JP.** Matched work high-intensity interval and continuous running induce similar increases in PGC-1α mRNA, AMPK, p38, and p53 phosphorylation in human skeletal muscle. *J Appl Physiol (1985)* 112: 1135–1143, 2012. doi:10.1152/japplphysiol.01040.2011.
4. **Brigelius-Flohé R, Flohé L.** Basic principles and emerging concepts in the redox control of transcription factors. *Antioxid Redox Signal* 15: 2335–2381, 2011. doi:10.1089/ars.2010.3534.
5. **Burgomaster KA, Howarth KR, Phillips SM, Rakobowchuk M, Macdonald MJ, McGee SL, Gibala MJ.** Similar metabolic adaptations during exercise after low volume sprint interval and traditional endurance training in humans. *J Physiol* 586: 151–160, 2008. doi:10.1113/jphysiol.2007.142109.
6. **Chae HZ, Kim HJ, Kang SW, Rhee SG.** Characterization of three isoforms of mammalian peroxiredoxin that reduce peroxides in the presence of thioredoxin. *Diabetes Res Clin Pract* 45: 101–112, 1999. doi:10.1016/S0168-8227(99)00037-6.
7. **Chen CL, Chen J, Rawale S, Varadharaj S, Kaumaya PP, Zweier JL, Chen YR.** Protein tyrosine nitration of the flavin subunit is associated with oxidative modification of mitochondrial complex II in the post-ischemic myocardium. *J Biol Chem* 283: 27991–28003, 2008. doi:10.1074/jbc.M802691200.
8. **Chen ZP, Stephens TJ, Murthy S, Canny BJ, Hargreaves M, Witters LA, Kemp BE, McConell GK.** Effect of exercise intensity on skeletal muscle AMPK signaling in humans. *Diabetes* 52: 2205–2212, 2003. doi:10.2337/diabetes.52.9.2205.
9. **Cobley JN, Sakellariou GK, Owens DJ, Murray S, Waldron S, Gregson W, Fraser WD, Burniston JG, Iwanejko LA, McArdle A, Morton JP, Jackson MJ, Close GL.** Lifelong training preserves some redox-regulated adaptive responses after an acute exercise stimulus in aged human skeletal muscle. *Free Radic Biol Med* 70: 23–32, 2014. doi:10.1016/j.freeradbiomed.2014.02.004.
10. **Combes A, Dekerle J, Webborn N, Watt P, Bougault V, Daussin FN.** Exercise-induced metabolic fluctuations influence AMPK, p38-MAPK and CaMKII phosphorylation in human skeletal muscle. *Physiol Rep* 3: e12462, 2015. doi:10.14814/phy2.12462.
11. **Cortassa S, O'Rourke B, Aon MA.** Redox-optimized ROS balance and the relationship between mitochondrial respiration and ROS. *Biochim Biophys Acta* 1837: 287–295, 2014. doi:10.1016/j.bbabio.2013.11.007.
12. **Daussin FN, Zoll J, Dufour SP, Ponsot E, Lonsdorfer-Wolf E, Doutreleau S, Mettauer B, Piquard F, Geny B, Richard R.** Effect of interval versus continuous training on cardiorespiratory and mitochondrial functions: relationship to aerobic performance improvements in sedentary subjects. *Am J Physiol Regul Integr Comp Physiol* 295: R264–R272, 2008. doi:10.1152/ajpregu.00875.2007.
13. **Dębski D, Smulik R, Zielonka J, Michałowski B, Jakubowska M, Dębowska K, Adamus J, Marcinek A, Kalyanaraman B, Sikora A.** Mechanism of oxidative conversion of Amplex Red to resorufin: ulse radiolysis and enzymatic studies. *Free Radic Biol Med* 95: 323–332, 2016. doi:10.1016/j.freeradbiomed.2016.03.027.
14. **Dimauro I, Mercatelli N, Caporossi D.** Exercise-induced ROS in heat shock proteins response. *Free Radic Biol Med* 98: 46–55, 2016. doi:10.1016/j.freeradbiomed.2016.03.028.
15. **Done AJ, Traustadóttir T.** Nrf2 mediates redox adaptations to exercise. *Redox Biol* 10: 191–199, 2016. doi:10.1016/j.redox.2016.10.003.
16. **Drake JC, Wilson RJ, Yan Z.** Molecular mechanisms for mitochondrial adaptation to exercise training in skeletal muscle. *FASEB J* 30: 13–22, 2016. doi:10.1096/fj.15-276337.
17. **Dröse S, Brandt U, Wittig I.** Mitochondrial respiratory chain complexes as sources and targets of thiol-based redox-regulation. *Biochim Biophys Acta* 1844: 1344–1354, 2014. doi:10.1016/j.bbapap.2014.02.006.
18. **Egan B, Carson BP, Garcia-Roves PM, Chibalin AV, Sarsfield FM, Barron N, McCaffrey N, Moyna NM, Zierath JR, O'Gorman DJ.** Exercise intensity-dependent regulation of peroxisome proliferator-activated receptor γ coactivator-α 1 mRNA abundance is associated with differential activation of upstream signalling kinases in human skeletal muscle. *J Physiol* 588: 1779–1790, 2010. doi:10.1113/jphysiol.2010.188011.
19. **Fisher-Wellman KH, Neufer PD.** Linking mitochondrial bioenergetics to insulin resistance via redox biology. *Trends Endocrinol Metab* 23: 142–153, 2012. doi:10.1016/j.tem.2011.12.008.
20. **Fu MH, Maher AC, Hamadeh MJ, Ye C, Tarnopolsky MA.** Exercise, sex, menstrual cycle phase, and 17β-estradiol influence metabolism-related genes in human skeletal muscle. *Physiol Genomics* 40: 34–47, 2009. doi:10.1152/physiolgenomics.00115.2009.
21. **Garber CE, Blissmer B, Deschenes MR, Franklin BA, Lamonte MJ, Lee I-M, Nieman DC, Swain DP; American College of Sports Medicine.** American College of Sports Medicine position stand. Quantity and quality of exercise for developing and maintaining cardiorespiratory, musculoskeletal, and neuromotor fitness in apparently healthy adults: guidance for prescribing exercise. *Med Sci Sports Exerc* 43: 1334–1359, 2011. doi:10.1249/MSS.0b013e318213fefb.
22. **Gibala MJ, Little JP, van Essen M, Wilkin GP, Burgomaster KA, Safdar A, Raha S, Tarnopolsky MA.** Short-term sprint interval versus traditional endurance training: similar initial adaptations in human skeletal muscle and exercise performance. *J Physiol* 575: 901–911, 2006. doi:10.1113/jphysiol.2006.112094.
23. **Gill RM, O'Brien M, Young A, Gardiner D, Mailloux RJ.** Protein S-glutathionylation lowers superoxide/hydrogen peroxide release from skeletal muscle mitochondria through modification of complex I and

inhibition of pyruvate uptake. *PLoS One* 13: e0192801, 2018. doi:10.1371/journal.pone.0192801.

24. **Goncalves RL, Quinlan CL, Perevoshchikova IV, Hey-Mogensen M, Brand MD.** Sites of superoxide and hydrogen peroxide production by muscle mitochondria assessed ex vivo under conditions mimicking rest and exercise. *J Biol Chem* 290: 209–227, 2015. doi:10.1074/jbc.M114.619072.
25. **Granata C, Oliveira RS, Little JP, Renner K, Bishop DJ.** Sprint-interval but not continuous exercise increases PGC-1α protein content and p53 phosphorylation in nuclear fractions of human skeletal muscle. *Sci Rep* 7: 44227, 2017. doi:10.1038/srep44227.
26. **Hawley JA, Noakes TD.** Peak power output predicts maximal oxygen uptake and performance time in trained cyclists. *Eur J Appl Physiol Occup Physiol* 65: 79–83, 1992. doi:10.1007/BF01466278.
27. **Hickey AJ, Renshaw GM, Speers-Roesch B, Richards JG, Wang Y, Farrell AP, Brauner CJ.** A radical approach to beating hypoxia: depressed free radical release from heart fibres of the hypoxia-tolerant epaulette shark (*Hemiscyllum ocellatum*). *J Comp Physiol B* 182: 91–100, 2012. doi:10.1007/s00360-011-0599-6.
28. **Hüttemann M, Lee I, Samavati L, Yu H, Doan JW.** Regulation of mitochondrial oxidative phosphorylation through cell signaling. *Biochim Biophys Acta* 1773: 1701–1720, 2007. doi:10.1016/j.bbamcr.2007.10.001.
29. **Irrcher I, Ljubicic V, Hood DA.** Interactions between ROS and AMP kinase activity in the regulation of PGC-1α transcription in skeletal muscle cells. *Am J Physiol Cell Physiol* 296: C116–C123, 2009. doi:10.1152/ajpcell.00267.2007.
30. **Jackson MJ.** Reactive oxygen species and redox-regulation of skeletal muscle adaptations to exercise. *Philos Trans R Soc Lond B Biol Sci* 360: 2285–2291, 2005. doi:10.1098/rstb.2005.1773.
31. **Jackson MJ.** Redox regulation of muscle adaptations to contractile activity and aging. *J Appl Physiol (1985)* 119: 163–171, 2015. doi:10.1152/japplphysiol.00760.2014.
32. **Kopprasch S, Srirangan D, Bergmann S, Graessler J, Schwarz PE, Bornstein SR.** Association of systemic oxidative stress and insulin resistance/sensitivity indices–the PREDIAS study. *Clin Endocrinol (Oxf)* 84: 48–54, 2015. doi:10.1111/cen.12811.
33. **Kramer PA, Duan J, Qian WJ, Marcinek DJ.** The measurement of reversible redox dependent post-translational modifications and their regulation of mitochondrial and skeletal muscle function. *Front Physiol* 6: 347, 2015. doi:10.3389/fphys.2015.00347.
34. **Krumschnabel G, Fontana-Ayoub M, Sumbalova Z, Heidler J, Gauper K, Fasching M, Gnaiger E.** Simultaneous high-resolution measurement of mitochondrial respiration and hydrogen peroxide production. *Methods Mol Biol* 1264: 245–261, 2015. doi:10.1007/978-1-4939-2257-4_22.
35. **Kruse R, Pedersen AJ, Kristensen JM, Petersson SJ, Wojtaszewski JF, Højlund K.** Intact initiation of autophagy and mitochondrial fission by acute exercise in skeletal muscle of patients with Type 2 diabetes. *Clin Sci (Lond)* 131: 37–47, 2016. doi:10.1042/CS20160736.
36. **Kubli DA, Quinsay MN, Huang C, Lee Y, Gustafsson ÅB.** Bnip3 functions as a mitochondrial sensor of oxidative stress during myocardial ischemia and reperfusion. *Am J Physiol Heart Circ Physiol* 295: H2025–H2031, 2008. doi:10.1152/ajpheart.00552.2008.
37. **Leckey JJ, Hoffman NJ, Parr EB, Devlin BL, Trewin AJ, Stepto NK, Morton JP, Burke LM, Hawley JA.** High dietary fat intake increases fat oxidation and reduces skeletal muscle mitochondrial respiration in trained humans. *FASEB J* 32: 2979–2991, 2018. doi:10.1096/fj.201700993R.
38. **Lee-Young RS, Canny BJ, Myers DE, McConell GK.** AMPK activation is fiber type specific in human skeletal muscle: effects of exercise and short-term exercise training. *J Appl Physiol (1985)* 107: 283–289, 2009. doi:10.1152/japplphysiol.91208.2008.
39. **Livak KJ, Schmittgen TD.** Analysis of relative gene expression data using real-time quantitative PCR and the 2(-Δ C(T)) method. *Methods* 25: 402–408, 2001. doi:10.1006/meth.2001.1262.
40. **MacInnis MJ, Zacharewicz E, Martin BJ, Haikalis ME, Skelly LE, Tarnopolsky MA, Murphy RM, Gibala MJ.** Superior mitochondrial adaptations in human skeletal muscle after interval compared to continuous single-leg cycling matched for total work. *J Physiol* 595: 2955–2968, 2017. doi:10.1113/JP272570.
41. **Mailloux RJ, Harper ME.** Uncoupling proteins and the control of mitochondrial reactive oxygen species production. *Free Radic Biol Med* 51: 1106–1115, 2011. doi:10.1016/j.freeradbiomed.2011.06.022.
42. **Mailloux RJ, Jin X, Willmore WG.** Redox regulation of mitochondrial function with emphasis on cysteine oxidation reactions. *Redox Biol* 2: 123–139, 2014. doi:10.1016/j.redox.2013.12.011.
43. **Mailloux RJ, Seifert EL, Bouillaud F, Aguer C, Collins S, Harper ME.** Glutathionylation acts as a control switch for uncoupling proteins UCP2 and UCP3. *J Biol Chem* 286: 21865–21875, 2011. doi:10.1074/jbc.M111.240242.
44. **Milne KJ, Noble EG.** Exercise-induced elevation of HSP70 is intensity dependent. *J Appl Physiol (1985)* 93: 561–568, 2002. doi:10.1152/japplphysiol.00528.2001.
45. **Miwa S, Treumann A, Bell A, Vistoli G, Nelson G, Hay S, von Zglinicki T.** Carboxylesterase converts Amplex red to resorufin: Implications for mitochondrial H2O2 release assays. *Free Radic Biol Med* 90: 173–183, 2016. doi:10.1016/j.freeradbiomed.2015.11.011.
46. **Murphy MP.** How mitochondria produce reactive oxygen species. *Biochem J* 417: 1–13, 2009. doi:10.1042/BJ20081386.
47. **Murphy RM, Lamb GD.** Important considerations for protein analyses using antibody based techniques: down-sizing Western blotting up-sizes outcomes. *J Physiol* 591: 5823–5831, 2013. doi:10.1113/jphysiol.2013.263251.
48. **Nguyen T, Huang HC, Pickett CB.** Transcriptional regulation of the antioxidant response element. Activation by Nrf2 and repression by MafK. *J Biol Chem* 275: 15466–15473, 2000. doi:10.1074/jbc.M000361200.
49. **Parker L, Shaw CS, Stepto NK, Levinger I.** Exercise and glycemic control: focus on redox homeostasis and redox-sensitive protein signaling. *Front Endocrinol (Lausanne)* 8: 87, 2017. doi:10.3389/fendo.2017.00087.
50. **Parker L, Trewin A, Levinger I, Shaw CS, Stepto NK.** Exercise-intensity dependent alterations in plasma redox status do not reflect skeletal muscle redox-sensitive protein signaling. *J Sci Med Sport* 21: 416–421, 2018. doi:10.1016/j.jsams.2017.06.017.
51. **Parker L, Trewin A, Levinger I, Shaw CS, Stepto NK.** The effect of exercise-intensity on skeletal muscle stress kinase and insulin protein signaling. *PLoS One* 12: e0171613, 2017. doi:10.1371/journal.pone.0171613.
52. **Picard M, Benoit J, Gentil BJ, McManus MJ, White K, St. Louis K, Gartside SE, Wallace DC, Turnbull DM.** Acute exercise remodels mitochondrial membrane interactions in mouse skeletal muscle. *J Appl Physiol (1985)* 115: 1562–1571, 2013. doi:10.1152/japplphysiol.00819.2013.
53. **Powers SK, Duarte J, Kavazis AN, Talbert EE.** Reactive oxygen species are signalling molecules for skeletal muscle adaptation. *Exp Physiol* 95: 1–9, 2010. doi:10.1113/expphysiol.2009.050526.
54. **Putman CT, Jones NL, Lands LC, Bragg TM, Hollidge-Horvat MG, Heigenhauser GJ.** Skeletal muscle pyruvate dehydrogenase activity during maximal exercise in humans. *Am J Physiol Endocrinol Metab* 269: E458–E468, 1995.
55. **Sakellariou GK, Vasilaki A, Palomero J, Kayani A, Zibrik L, McArdle A, Jackson MJ.** Studies of mitochondrial and nonmitochondrial sources implicate nicotinamide adenine dinucleotide phosphate oxidase(s) in the increased skeletal muscle superoxide generation that occurs during contractile activity. *Antioxid Redox Signal* 18: 603–621, 2013. doi:10.1089/ars.2012.4623.
56. **Salo DC, Donovan CM, Davies KJ.** HSP70 and other possible heat shock or oxidative stress proteins are induced in skeletal muscle, heart, and liver during exercise. *Free Radic Biol Med* 11: 239–246, 1991. doi:10.1016/0891-5849(91)90119-N.
57. **Scheele C, Nielsen S, Pedersen BK.** ROS and myokines promote muscle adaptation to exercise. *Trends Endocrinol Metab* 20: 95–99, 2009. doi:10.1016/j.tem.2008.12.002.
58. **Smolka MB, Zoppi CC, Alves AA, Silveira LR, Marangoni S, Pereira-Da-Silva L, Novello JC, Macedo DV.** HSP72 as a complementary protection against oxidative stress induced by exercise in the soleus muscle of rats. *Am J Physiol Regul Integr Comp Physiol* 279: R1539–R1545, 2000. doi:10.1152/ajpregu.2000.279.5.R1539.
59. **Song IK, Lee JJ, Cho JH, Jeong J, Shin DH, Lee KJ.** Degradation of redox-sensitive proteins including peroxiredoxins and DJ-1 is promoted by oxidation-induced conformational changes and ubiquitination. *Sci Rep* 6: 34432, 2016. doi:10.1038/srep34432.
60. **Strobel NA, Matsumoto A, Peake JM, Marsh SA, Peternelj TT, Briskey D, Fassett RG, Coombes JS, Wadley GD.** Altering the redox state of skeletal muscle by glutathione depletion increases the exercise-activation of PGC-1α. *Physiol Rep* 2: e12224, 2014. doi:10.14814/phy2.12224.

61. **Thompson JR, Swanson SA, Casale GP, Johanning JM, Papoutsi E, Koutakis P, Miserlis D, Zhu Z, Pipinos II.** Gastrocnemius mitochondrial respiration: are there any differences between men and women? *J Surg Res* 185: 206–211, 2013. doi:10.1016/j.jss.2013.05.054.
62. **Timpani CA, Trewin AJ, Stojanovska V, Robinson A, Goodman CA, Nurgali K, Betik AC, Stepto N, Hayes A, McConell GK, Rybalka E.** Attempting to compensate for reduced neuronal nitric oxide synthase protein with nitrate supplementation cannot overcome metabolic dysfunction but rather has detrimental effects in dystrophin-deficient mdx muscle. *Neurotherapeutics* 14: 429–446, 2017. doi:10.1007/s13311-016-0494-7.
63. **Tonkonogi M, Harris B, Sahlin K.** Mitochondrial oxidative function in human saponin-skinned muscle fibres: effects of prolonged exercise. *J Physiol* 510: 279–286, 1998. doi:10.1111/j.1469-7793.1998.279bz.x.
64. **Tonkonogi M, Walsh B, Tiivel T, Saks V, Sahlin K.** Mitochondrial function in human skeletal muscle is not impaired by high intensity exercise. *Pflugers Arch* 437: 562–568, 1999. doi:10.1007/s004240050818.
65. **Trewin AJ, Berry BJ, Wojtovich AP.** Exercise and mitochondrial dynamics: keeping in shape with ROS and AMPK. *Antioxidants* 7: E7, 2018. doi:10.3390/antiox7010007.
66. **Trewin AJ, Levinger I, Parker L, Shaw CS, Serpiello FR, Anderson MJ, McConell GK, Hare DL, Stepto NK.** Acute exercise alters skeletal muscle mitochondrial respiration and H2O2 emission in response to hyperinsulinemic-euglycemic clamp in middle-aged obese men. *PLoS One* 12: e0188421, 2017. doi:10.1371/journal.pone.0188421.
67. **Trewin AJ, Lundell LS, Perry BD, Patil KV, Chibalin AV, Levinger I, McQuade LR, Stepto NK.** Effect of *N*-acetylcysteine infusion on exercise-induced modulation of insulin sensitivity and signaling pathways in human skeletal muscle. *Am J Physiol Endocrinol Metab* 309: E388–E397, 2015. doi:10.1152/ajpendo.00605.2014.
68. **Vainshtein A, Tryon LD, Pauly M, Hood DA.** Role of PGC-1α during acute exercise-induced autophagy and mitophagy in skeletal muscle. *Am J Physiol Cell Physiol* 308: C710–C719, 2015. doi:10.1152/ajpcell.00380.2014.
69. **Votion DM, Fraipont A, Goachet AG, Robert C, van Erck E, Amory H, Ceusters J, de la Rebière de Pouyade G, Franck T, Mouithys-Mickalad A, Niesten A, Serteyn D.** Alterations in mitochondrial respiratory function in response to endurance training and endurance racing. *Equine Vet J Suppl* 42: 268–274, 2010. doi:10.1111/j.2042-3306.2010.00271.x.
70. **Wadley AJ, Aldred S, Coles SJ.** An unexplored role for Peroxiredoxin in exercise-induced redox signalling? *Redox Biol* 8: 51–58, 2016. doi:10.1016/j.redox.2015.10.003.
71. **Wadley GD, Nicolas MA, Hiam DS, McConell GK.** Xanthine oxidase inhibition attenuates skeletal muscle signaling following acute exercise but does not impair mitochondrial adaptations to endurance training. *Am J Physiol Endocrinol Metab* 304: E853–E862, 2013. doi:10.1152/ajpendo.00568.2012.
72. **Wang L, Psilander N, Tonkonogi M, Ding S, Sahlin K.** Similar expression of oxidative genes after interval and continuous exercise. *Med Sci Sports Exerc* 41: 2136–2144, 2009. doi:10.1249/MSS.0b013e3181abc1ec.
73. **Westerblad H, Bruton JD, Katz A.** Skeletal muscle: energy metabolism, fiber types, fatigue and adaptability. *Exp Cell Res* 316: 3093–3099, 2010. doi:10.1016/j.yexcr.2010.05.019.
74. **Wong HS, Dighe PA, Mezera V, Monternier PA, Brand MD.** Production of superoxide and hydrogen peroxide from specific mitochondrial sites under different bioenergetic conditions. *J Biol Chem* 292: 16804–16809, 2017. doi:10.1074/jbc.R117.789271.
75. **Zhang J, Ney PA.** Role of BNIP3 and NIX in cell death, autophagy, and mitophagy. *Cell Death Differ* 16: 939–946, 2009. doi:10.1038/cdd.2009.16.